This is a preprint, the final version is subject to change, of the American Mineralogist (MSA)
Cite as Authors (Year) Title. American Mineralogist, in press.
DOI: https://doi.org/10.2138/am-2019-6814

Revision 1

Meyrowitzite, $Ca(UO_2)(CO_3)_2 \cdot 5H_2O$, a new mineral with a novel uranyl-carbonate sheet

ANTHONY R. KAMPF[1§], JAKUB PLÁŠIL[2], TRAVIS A. OLDS[3], BARBARA P. NASH[4], JOE MARTY[5] AND HARVEY E. BELKIN[6]

[1]Mineral Sciences Department, Natural History Museum of Los Angeles County, 900 Exposition Boulevard, Los Angeles, CA 90007, USA

[2] Institute of Physics ASCR, v.v.i., Na Slovance 1999/2, 18221 Prague 8, Czech Republic

[3] Department of Civil and Environmental Engineering and Earth Sciences, University of Notre Dame, Notre Dame, IN 46556, USA

[4] Department of Geology and Geophysics, University of Utah, Salt Lake City, Utah 84112, USA

[5] 5199 East Silver Oak Road, Salt Lake City, UT 84108, USA

[6] United States Geological Survey (Ret.), Reston, VA 20190 USA

ABSTRACT

Meyrowitzite, $Ca(UO_2)(CO_3)_2 \cdot 5H_2O$, is a new mineral species from the Markey mine, Red Canyon, San Juan County, Utah, U.S.A. It is a secondary phase found on calcite-veined asphaltum in association with gypsum, markeyite, and rozenite. Meyrowitzite occurs as blades up to about 0.2 mm in length, elongate on [010], flattened on {100}, and exhibiting the forms {100}, {001}, {101}, {110}, and {011}. The mineral is yellow and transparent with vitreous luster and very pale yellow streak. Fluorescence is from weak greenish yellow to moderate greenish blue. The Mohs hardness is *ca* 2, tenacity is brittle, fracture is irregular,

§ Email: akampf@nhm.org

and there is one perfect cleavage, {-101}. The measured density is 2.70(2) g·cm^{-3}. The mineral is optically biaxial (+) with α = 1.520(2), β = 1.528(2), and γ = 1.561(2) (white light). The 2*V*(meas.) = 53.0(6)°; weak dispersion, *r* > *v*; optical orientation: *Z* = **b**, *Y* ^ **a** ≈ 19° in obtuse β; pleochroism pale yellow, *X* ≈ *Y* < *Z*. Electron microprobe analyses provided the empirical formula $Ca_{0.94}(U_{1.00}O_2)(CO_3)_2 \cdot 5(H_{2.02}O)$ on the basis of U = 1 and O = 13 *apfu*, as indicated by the crystal structure determination. Meyrowitzite is monoclinic, $P2_1/n$, *a* = 12.376(3), *b* = 16.0867(14), *c* = 20.1340(17) Å, β = 107.679(13)°, *V* = 3819.3(12) Å^3, and *Z* = 12. The structure (R_1 = 0.055 for 3559 $I_o > 2\sigma I$) contains both UO_7 pentagonal bipyramids and UO_8 hexagonal bipyramids, the later participating in uranyl tricarbonate clusters (UTC). The two kinds of bipyramids and the carbonate groups link to form a novel corrugated heteropolyhedral sheet. This is the first structural characterization of a uranyl-carbonate mineral with a U:C ratio of 1:2. Meyrowitzite is apparently dimorphous with zellerite.

Keywords: meyrowitzite; new mineral species; uranyl tricarbonate; crystal structure; zellerite; Markey mine, Red Canyon, Utah.

INTRODUCTION

Carbonate minerals containing U^{6+} are usually relatively soluble in aqueous solutions. Aqueous uranyl-carbonate complexes are generally quite stable and are responsible for uranium migration in the environment on a large scale (Langmuir, 1978; Clark *et al.*, 1995). The most abundant complexes are uranyl monocarbonate, $[(UO_2)(CO_3)]^0$, uranyl dicarbonate, $[(UO_2)(CO_3)_2]^{2-}$ and uranyl tricarbonate, $[(UO_2)(CO_3)_3]^{4-}$, with pK_a values of 5.5, 7 and 9, respectively (Langmuir, 1978). The most abundant uranyl carbonate minerals are those with a U:C ratio of 1:3, which crystallize from solutions of relatively high pH, from neutral to alkaline. However, very little data is available for minerals with a U:C ratio of 1:2; for

example, the mineral zellerite, $Ca[(UO_2)(CO_3)_2]\cdot 5H_2O$ (Coleman *et al.*, 1966), which occurs commonly within the carbonate-rich alteration associations of supergene U minerals, has so far eluded crystallographic characterization. Here, we present the description of the new uranyl-carbonate mineral, meyrowitzite, $Ca(UO_2)(CO_3)_2\cdot 5H_2O$, a dimorph of zellerite, and the first structural characterization of a uranyl-carbonate mineral with a U:C ratio of 1:2.

Meyrowitzite is named in honor of American analytical chemist Robert Meyrowitz (1916-2013). Mr. Meyrowitz received his bachelor's degree in chemistry from the City College of New York in 1936, after which he conducted research in microchemical analysis at Brooklyn College (New York). During World War II, he served in the U.S. Army and, because of his skills as a chemist, he was assigned to work on the Manhattan Project. After the war, he joined the United States Geological Survey (USGS), from which he retired in 1973. In his years at the USGS, he was especially known for his knack for developing innovative new methods for analyzing small and difficult to study mineralogical samples, and is also well-known for his formulation of the high-index immersion liquids (1.74 to 2.00) that are still in use for optical determinations (Meyrowitz and Larsen, 1951). He published prolifically, often collaborating on the descriptions of new minerals (e.g. brockite, duttonite, goldmanite, hendersonite, metazellerite, ningyoite, sahamalite, sherwoodite, simplotite, weeksite and zellerite). Many of the new minerals species that he worked on were from the uranium deposits of the western U.S. Among them was zellerite, the dimorph of the meyrowitzite. Robert Meyrowitz' son Alan has approved of the naming of the mineral in his father's honor.

The new mineral and name were approved by the Commission on New Minerals, Nomenclature and Classification of the International Mineralogical Association (IMA 2018-039). Two cotype specimens of meyrowitzite are deposited in the collections of the Natural History Museum of Los Angeles County, Los Angeles, California, USA, catalogue numbers

66789 and 66790.

OCCURRENCE

Meyrowitzite was discovered on specimens collected underground in the Markey mine, Red Canyon, White Canyon District, San Juan County, Utah, USA (37°32'57"N 110°18'08"W). The Markey mine is located about 1 km southwest of the Blue Lizard mine, on the east-facing side of Red Canyon, about 72 km west of the town of Blanding, Utah, and about 22 km southeast of Good Hope Bay on Lake Powell. The geology of the Markey mine is quite similar to that of the Blue Lizard mine (Chenoweth, 1993; Kampf, *et al.*, 2015a), although the secondary mineralogy of the Markey mine is notably richer in carbonate phases. The information following is taken largely from Chenoweth (1993).

Jim Rigg of Grand Junction, Colorado began staking claims in Red Canyon in March of 1949. The Markey group of claims, staked by Rigg and others, was purchased by the Anaconda Copper Mining Company on June 1, 1951. After limited exploration and production, the mine closed in 1955. The mine was subsequently acquired from Anaconda by Calvin Black of Blanding, Utah under whose ownership the mine operated from 1960 to 1982 and was a leading producer in the district for nearly that entire period.

Mineralized channels are in the Shinarump member of the Chinle Formation. The Shinarump member consists of medium- to coarse-grained sandstone, conglomeratic sandstone beds and thick siltstone lenses. Ore minerals were deposited as replacements of wood and other organic material and as disseminations in the enclosing sandstone. Since the mine closed, oxidation of primary ores in the humid underground environment has produced a variety of secondary minerals, mainly sulfates, as efflorescent crusts on the surfaces of mine walls.

Meyrowitzite is a very rare mineral, found on calcite-veined asphaltum in association

with gypsum, markeyite (Kampf *et al*., 2018) and rozenite. See Kampf *et al*. (2018) for a more complete list of the secondary minerals identified from the Markey mine, including several which are recently described new species.

PHYSICAL AND OPTICAL PROPERTIES

Crystals of meyrowitzite are blades up to about 0.2 mm in length, commonly in irregular and radiating intergrowths (Fig. 1). Blades are elongate on [010], flattened on {100} and exhibit the forms {100}, {001}, {101}, {110} and {011} (Fig. 2). No twinning was observed. The mineral is yellow and transparent with vitreous luster and very pale-yellow streak. Meyrowitzite exhibits variable fluorescence from weak greenish yellow to moderate greenish blue under a 405 nm laser. It has a Mohs hardness of about 2, brittle tenacity, irregular fracture, and one perfect cleavage on {-101}. The density measured by flotation in a mixture of methylene iodide and toluene is 2.70(2) $g \cdot cm^{-3}$. The calculated density is 2.702 $g \cdot cm^{-3}$ using the empirical formula and 2.714 $g \cdot cm^{-3}$ using the ideal formula. The mineral is easily soluble in H_2O at room temperature.

Meyrowitzite is optically biaxial (+) with $\alpha = 1.520(2)$, $\beta = 1.528(2)$, and $\gamma = 1.561(2)$ measured in white light. The $2V$ measured using extinction data analyzed with EXCALIBRW (Gunter *et al*., 2004) is 53.0(6)°; the calculated $2V$ is 53.3°. The dispersion is weak, $r > v$. The optical orientation is $Z =$ **b**, $Y \wedge$ **a** ≈ 19° in obtuse β. Crystals are weakly pleochroic in shades of pale yellow, $X \approx Y < Z$. The Gladstone–Dale compatibility, $1 - (K_P/K_C)$, (Mandarino, 2007) is -0.039 (excellent) using the empirical formula, and -0.035 (excellent) using the ideal formula – where $k(UO_3) = 0.134$ as provided by Larsen (1921).

RAMAN SPECTROSCOPY

Raman spectroscopy was conducted on a Horiba XploRA PLUS. Because of

significant fluorescence using a 532 nm diode laser, the spectrum was recorded using a 785 nm diode laser. The spectrum from 1800 to 80 cm^{-1} is shown in Figure 3. In general, the measured meyrowitzite spectrum is similar to the spectrum of zellerite (Frost *et al.*, 2008); however, the spectrum of meyrowitzite contains larger number of bands (especially in the region of UO_2^{2+} stretching vibrations), most probably due to lowering of the corresponding site-symmetry: orthorhombic (zellerite) → monoclinic (meyrowitzite).

A broad band composed of two overlapping bands at 1450 and 1380 cm^{-1} results from the split doubly degenerate ν_3 $(CO_3)^{2-}$ antisymmetric stretching vibrations of the $(CO_3)^{2-}$ polyhedra. Medium to strong bands at 1100, 1095, 1080, and 1065cm^{-1} are associated with the ν_1 $(CO_3)^{2-}$ symmetric stretching vibrations. Splitting of these bands is consistent with the presence of structurally non-equivalent carbonate units (Koglin *et al*., 1979; Anderson *et al*., 1980; Čejka, 1999 and 2005, and references therein); there are six independent C sites in the structure of meyrowitzite (see below). A multi-component band of high intensity, composed of overlapping bands at 850, 840, 835, and 825 cm^{-1}, is attributable to the ν_2 (δ) $(CO_3)^{2-}$ bending vibrations, and (in overlap) to the ν_1 $(UO_2)^{2+}$ symmetric stretching vibrations. Using the empirical relation of Bartlett and Cooney (1989), we can infer the corresponding U–O bond lengths from the above-mentioned wavenumbers (in the order as given above): 1.76, 1.77, 1.78, and 1.79 Å. The structure refinement provided U–O bond-lengths in the range of 1.75–1.80 Å; therefore, it is possible that all observed overlapping bands in the region 850–825 cm^{-1} belong to the ν_1 $(UO_2)^{2+}$ symmetric stretching vibration. A strong component band, composed of overlapping bands at 760 and 745 cm^{-1}, and a weak composite band at 687 cm^{-1} are attributable to the ν_4 (δ) $(CO_3)^{2-}$ bending vibrations. Medium to strong bands at 270 and 240 cm^{-1} are attributable to split doubly degenerate ν_2 (δ) $(UO_2)^{2+}$ bending vibrations. Medium-strong bands at 218, 145, and 125 cm^{-1} are attributable to the lattice modes (Koglin *et al*., 1979; Anderson *et al*., 1980; Čejka, 1999 and 2005).

This is a preprint, the final version is subject to change, of the American Mineralogist (MSA)
Cite as Authors (Year) Title. American Mineralogist, in press.
DOI: https://doi.org/10.2138/am-2019-6814

CHEMICAL ANALYSIS

Chemical analyses (3) were performed at the University of Utah on a Cameca SX-50 electron microprobe with four wavelength dispersive spectrometers and using Probe for EPMA software (Probe Software, Inc., Eugene, OR). Analytical conditions were 15 keV accelerating voltage, 10 nA beam current and a beam diameter of 5 μm. Raw X-ray intensities were corrected for matrix effects with a $\phi\rho(z)$ algorithm (Pouchou and Pichoir, 1991). Concentrations of total oxygen and carbon, calculated from the ideal formula, were used in the matrix correction.

It was impossible to obtain a good polish and crystal surfaces suffered further because of crystal dehydration; however, the beam produced no damage to the sample. Because insufficient material is available for direct determination of H_2O and CO_2, they are calculated based upon the structure determination (2 C and 13 O *apfu*). Analytical data are given in Table 1. The empirical formula is $Ca_{0.94}(U_{1.00}O_2)(CO_3)_2 \cdot 5(H_{2.02}O)$. The ideal formula is $Ca(UO_2)(CO_3)_2 \cdot 5H_2O$, which requires CaO 10.78, UO_3 54.98, CO_2 16.92, and H_2O 17.32, total 100 wt.%.

X-RAY CRYSTALLOGRAPHY AND STRUCTURE DETERMINATION

Both powder and single-crystal X-ray studies were carried out using a Rigaku R-Axis Rapid II curved imaging plate microdiffractometer with monochromatized Mo$K\alpha$ radiation. For the powder study, a Gandolfi-like motion on the φ and ω axes was used to randomize the sample, which consisted of several crystals. Observed *d* values and intensities were derived by profile fitting using JADE 2010 software (Materials Data, Inc. Livermore, CA). Data are given in Table 2. Unit cell parameters refined from the powder data using JADE 2010 with

whole pattern fitting are a = 12.417(17), b = 16.127(17), c = 20.123(17) Å, β = 107.53(4)° and V = 3842 (7) Å^3.

Crystals of meyrowitzite are of relatively poor quality for single-crystal study. The best crystal fragment, which was used for the collection of structure data, exhibited significant mosaicity, some spot streaking and some extra spots indicative of one or more satellite crystals. This fragment, measuring only 80 × 80 × 30 μm, provided usable data only to a resolution of 0.88 Å. The Rigaku CrystalClear software package was used for processing the structure data, including Lorentz and polarization corrections, and the application of an empirical absorption correction using the multi-scan method with ABSCOR (Higashi, 2001). The space group $P2_1/n$ was suggested by the Rigaku XPlain program, which readily led to a structure solution using SIR2011 (Burla *et al*., 2012). It should be noted that numerous reflections violated the extinction conditions for space group $P2_1/n$, and particularly for the n glide; however, efforts to obtain viable structure models in other space groups were unsuccessful. We attribute the space-group violations to the imperfect nature of the crystal fragment, as noted above, and this also led us to omit five poorly fitting reflections that did not violate the extinction conditions. SHELXL-2013 (Sheldrick, 2015) was used for the refinement of the structure. The limited data set allowed refinement with anisotropic displacement parameters for all fully occupied sites, but not for four approximately half-occupied H_2O sites (OW14, OW15, OW16 and OW17). It also did not allow the location of H sites in difference Fourier maps. Data collection and refinement details are given in Table 3, atom coordinates and displacement parameters in Table 4, selected bond distances in Table 5 and a bond valence analysis in Table 6.

DISCUSSION

There are three U sites in the structure of meyrowitzite. Two (U1 and U2) are surrounded by eight O atoms forming a squat UO_8 hexagonal bipyramid; the other (U3) is surrounded by seven O atoms forming a squat UO_7 pentagonal bipyramid. The two short apical bonds of all three bipyramids constitute the UO_2^{2+} uranyl group. Of the six CO_3^{2-} groups in the structure, three centered by C1, C2 and C3 share alternating equatorial edges of the U1 hexagonal bipyramid, thereby forming the well-known uranyl tricarbonate (UTC) unit. The other three, centered by C4, C5 and C6, share alternating equatorial edges of the U2 hexagonal bipyramid, forming a second UTC unit. The five equatorial corners of the U3 pentagonal bipyramid are shared with O atoms of the C1, C2, C3, C4 and C6 carbonate groups. These linkages create a unique corrugated uranyl carbonate heteropolyhedral sheet parallel to {10-1} (Figure 5). The U2 UTCs are oriented perpendicular to the plane of the sheet (Figure 6) with the unshared corner of the C5 carbonate group pointing away from the sheet. Three Ca atoms (Ca1, Ca2 and Ca3) are eight-coordinated to O atoms in the sheets and to OW atoms, although Ca3 is effectively only seven-coordinated because two of its ligands (OW15 and OW16) are only half-occupied. The Ca polyhedra do not link to one another; instead, they share edges and corners with the polyhedra in the uranyl carbonate heteropolyhedral sheets, thereby linking the sheets into a framework (Figure 7). The fully occupied OW9 through OW13 sites and the half-occupied OW14 and OW17 sites are located in the cavities in this framework.

Minerals with structures containing both UO_7 pentagonal bipyramid and UO_8 hexagonal bipyramid are rare. Other examples include ewingite, $Mg_8Ca_8(UO_2)_{24}(CO_3)_{30}O_4(OH)_{12}(H_2O)_{138}$, (Olds *et al*., 2017) and fontanite, $Ca[(UO_2)_3(CO_3)_2O_2](H_2O)_6$, (Hughes and Burns, 2003). The structure of ewingite is based on a large and complex uranyl carbonate polyhedral cluster that bears no similarity to the structure of meyrowitzite. Fontanite has uranyl carbonate sheets that are linked by CaO_8

polyhedra; however, the UO_7 and UO_8 polyhedra form edge-sharing chains within these sheets and there are no UTC units, but rather uranyl dicarbonate units.

Meyrowitzite has a crystal structure based on a unique corrugated uranyl carbonate heteropolyhedral sheet. Meyrowitzite is apparently dimorphous with zellerite (Coleman *et al*., 1966); however, the structure of zellerite is not known. The PXRD patterns for meyrowitzite and zellerite, compared graphically in Figure 4, are quite different. Although the strongest peaks in the zellerite pattern are represented in the meyrowitzite pattern, the four strongest lines in the meyrowitzite pattern are not in the zellerite pattern. Comparative data for meyrowitzite and zellerite are provided in Table 7. In the Strunz system, meyrowitzite and zellerite both belong in class 5.EB: uranyl carbonates with UO_2:CO_3 > 1:1 to 1:2.

IMPLICATIONS

Numerous studies conducted over the past 50 years have led to a well-developed understanding of the geochemistry of U-CO_3 systems (Langmuir, 1978; Chopin and Jensen, 2010; Maher *et al.*, 2013). All acknowledge that carbonate binds to uranium strongly and that uranyl-carbonate complexes are among those most relevant to the environmental chemistry of uranium. One of the most common species, the uranyl-tricarbonate complex (UTC), is exceptionally stable in aqueous solutions and it is known to occur in 33 different uranyl-carbonate minerals. Significant evidence suggests that additional polymeric UTC-hydrolyzed U complexes are prevalent species in some systems (Müller *et al*., 2008; Saini *et al*., 1989; Ciavatta *et al*., 1980), and this combination is known in several exceptionally rare minerals, including fontanite, $Ca[(UO_2)_3(CO_3)_2O_2](H_2O)_6$ (Hughes and Burns, 2003), roubaultite, $Cu_2(UO_2)_3(CO_3)_2O_2(OH)_2(H_2O)_4$ (Ginderow and Cesbron, 1985), wyartite, $Ca(CO_3)[U^{5+}(U^{6+}O_2)_2O_4(OH)](H_2O)_7$ (Burns and Finch, 1999), bijvoetite-Y $[Y_8(H_2O)_{25}(UO_2)_{16}O_8(OH)_8(CO_3)_{16}](H_2O)_{14}$ (Li *et al.*, 2000), kamotoite-(Y),

249 $Y_2(UO_2)_4O_2(OH)_2(CO_3)_4(H_2O)_{12.54}$ (Plášil and Petříček, 2017), above-mentioned ewingite
250 (Olds *et al.*, 2017), and herein with the description of meyrowitzite. The structure of ewingite
251 suggests that relatively large polynuclear species containing hydrolyzed uranium and UTC
252 may have assembled in solution prior to crystal growth, or possibly at the crystal-solution
253 interface. Though we recognize the conditions required for their formation are very narrow,
254 these minerals reveal definite gaps in our understanding of uranyl-carbonate-hydroxide
255 equilibria that can be better determined through crystal-chemical studies of natural systems.
256 Crystallization of these minerals offers a diagnostic view into the conditions and speciation of
257 the solutions from which they crystallize. These missing data are necessary for producing
258 accurate models of contamination speciation in repositories for nuclear waste.

259 The fact that meyrowitzite contains a heretofore-unreported type of uranyl-carbonate
260 heteropolyhedral sheet makes its reported occurrence in a natural setting of significant
261 importance in expanding our understanding of uranyl-carbonate interactions in natural
262 systems. Furthermore, although based upon composition alone, meyrowitzite, with a U:C ratio
263 of 1:2, might have been expected to contain the uranyl-dicarbonate complex, $[(UO_2)(CO_3)_2]^{2-}$,
264 it is noteworthy that the determination of its structure shows it to contain instead a uranyl-
265 tricarbonate complex. Based upon this, it is reasonable to conjecture that its dimorph zellerite
266 may also contain a uranyl-tricarbonate complex, rather than a uranyl-dicarbonate complex.
267

268 **ACKNOWLEDGEMENTS**

269 Two anonymous reviewers and the Technical Editor are thanked for constructive
270 comments, which improved the manuscript. Associate Editor G. Diego Gatta is thanked for
271 shepherding the manuscript through the review process. Alan Meyrowitz is thanked for
272 providing background information about his father, Robert Meyrowitz. This study was

funded, in part, by the John Jago Trelawney Endowment to the Mineral Sciences Department of the Natural History Museum of Los Angeles County.

REFERENCES

Anderson A., Chieh Ch., Irish D.E., and Tong J.P.K. (1980) An X-ray crystallographic, Raman, and infrared spectral study of crystalline potassium uranyl carbonate, $K_4UO_2(CO_3)_3$. *Canadian Journal of Chemistry*, **58**, 1651–1658.

Bartlett, J.R. and Cooney, R.P. (1989) On the determination of uranium-oxygen bond lengths in dioxouranium(VI) compounds by Raman spectroscopy. *Journal of Molecular Structure*, **193**, 295–300.

Burla, M. C., Caliandro, R., Camalli, M., Carrozzini, B., Cascarano, G.L., Giacovazzo, C., Mallamo, M., Mazzone, A., Polidori, G., and Spagna, R. (2012) *SIR2011*: a new package for crystal structure determination and refinement. *Journal of Applied Crystallography*, **45**, 357–361.

Burns, P.C. and Finch, R.J. (1999) Wyartite: crystallographic evidence for the first pentavalent-uranium mineral. *American Mineralogist*, **84**, 1456–1460.

Čejka J. (1999) Infrared and thermal analysis of the uranyl minerals. *Reviews in Mineralogy*, **38**, 521–622.

Čejka J. (2005) Vibrational spectroscopy of the uranyl minerals – infrared and Raman spectra of the uranyl minerals. II. Uranyl carbonates. *Bulletin mineralogicko-petrologického oddělení Národního muzea (Praha)*, **13**, 62–72 (in Czech).

Chenoweth, W.L. (1993) The Geology and Production History of the Uranium Deposits in the White Canyon Mining District, San Juan County, Utah. *Utah Geological Survey Miscellaneous Publication*, **93**–**3**.

Choppin, G. R. and Jensen, M. P. (2010) Actinides in Solution: Complexation and Kinetics. In Morss, L. R., Edelstein, N. M. and Fuger, J. (eds) *The Chemistry of the Actinide and Transactinide Elements*, 4th edition. Springer, Dordrecht, the Netherlands, pp. 2524−2621.

Ciavatta, L., Ferri, D., Grenthe, I., and Salvatore, F. (1981) The first acidification step of the tris(carbonato)dioxouranate(VI) ion, $UO_2(CO_3)_3^{4-}$. *Inorganic Chemistry*, **20**, 463–467.

Coleman, R.G., Ross, D.R., and Meyrowitz, R. (1966) Zellerite and metazellerite, new uranyl carbonates. *American Mineralogist*, **51**, 1567–1578.

Ferraris, G. and Ivaldi, G. (1988) Bond valence vs. bond length in O…O hydrogen bonds. *Acta Crystallographica*, **B44**, 341–344.

Frost, R.L., Dickfos, M.J., and Čejka, J. (2008) Raman spectroscopic study of the uranyl carbonate mineral zellerite. *Journal of Raman Spectroscopy*, **39**, 582–586.

Gagné, O.C. and Hawthorne, F.C (2015) Comprehensive derivation of bond-valence parameters for ion pairs involving oxygen. *Acta Crystallographica*, **B71**, 562–578.

Ginderow, D. and Cesbron, F. (1985) The structure of roubaultite, $Cu_2(UO_2)_3(CO_3)_2O_2(OH)_2{\cdot}4H_2O$. *Acta Crystallographica*, **C41**, 654–657.

Gunter, M.E., Bandli, B.R., Bloss, F.D., Evans, S.H., Su, S.C., and Weaver, R. (2004) Results from a McCrone spindle stage short course, a new version of EXCALIBR, and how to build a spindle stage. *The Microscope*, **52**, 23-39.

Higashi, T. (2001) *ABSCOR*. Rigaku Corporation, Tokyo.

Hughes, K.-A. and Burns, P.C. (2003) A new uranyl carbonate sheet in the crystal structure of fontanite, $Ca[(UO_2)_3(CO_3)_2O_2](H_2O)_6$. *American Mineralogist*, **88**, 962–966.

Kampf, A.R., Kasatkin, A.V., Čejka, J., and Marty, J. (2015) Plášilite, $Na(UO_2)(SO_4)(OH){\cdot}2H_2O$, a new uranyl sulfate mineral from the Blue Lizard mine, San Juan County, Utah, USA. *Journal of Geosciences*, **60**, 1–10.

321 Kampf, A.R., Plášil, J., Kasatkin, A.V., Marty, J., and Čejka, J. (2018) Markeyite, a new
322 calcium uranyl tricarbonate mineral from the Markey mine, San Juan County, Utah, USA.
323 *Mineralogical Magazine* **82**, (in press)
324 Koglin E., Schenk H.J., and Schwochau K. (1979) Vibrational and low temperature optical
325 spectra of the uranyl tricarbonato complex $[UO_2(CO_3)_3]^{4-}$. *Spectrochimica Acta*, **35A**,
326 641–647.
327 Langmuir, D. (1978) Uranium solution–mineral equilibria at low temperatures with
328 applications to sedimentary ore. *Geochimica et Cosmochimica Acta*, **42**, 547–569.
329 Larsen, E.S. (1921) The microscopic determination of the nonopaque minerals. U.S.
330 Geological Survey, Bulletin 679.
331 Li, Y., Burns, P.C., and Gault, R.A. (2000) A new rare earth-element uranyl carbonate sheet
332 in the structure of bijvoetite. *Canadian Mineralogist*, **38**, 153–162.
333 Maher, K., Bargar, J.R., and Brown, G.E., Jr. (2013) Environmental speciation of actinides.
334 *Inorganic Chemistry*, **52**, 3510–3532.
335 Mandarino, J.A. (2007) The Gladstone–Dale compatibility of minerals and its use in selecting
336 mineral species for further study. Canadian Mineralogist, 45, 1307-1324.
337 Meyrowitz, R. and Larsen, E.S., Jr. (1951) Immersion liquids of high refractive index.
338 *American Mineralogist*, **36**, 746–750.
339 Müller, K., Brendler, V., and Foerstendorf, H. (2008) Aqueous uranium(VI) hydrolysis
340 species characterized by attenuated total reflection Fourier-transform infrared
341 spectroscopy. *Inorganic Chemistry*, **47**, 10127–10134.
342 Olds, T.A., Plášil, J., Kampf, A.R., Burns, P.C., Simonetti, A., and Sadergaski, L.R. (2017)
343 Ewingite: Earth's most complex mineral. *Geology*, **45**, 1007–1010.
344 Olds, T., Sadergaski, L.R., Plášil, J., Kampf, A.R., Burns, P., Steele, I.M., Marty, J., Carlson,
345 S.M., and Mills, O.P. (2017) Leószilárdite, the first Na,Mg-containing uranyl carbonate

346 from the Markey Mine, San Juan County, Utah, USA. *Mineralogical Magazine* **81**, 743–
347 754.
348 Plášil, J. and Petříček, V. (2017) Crystal structure of the (*REE*)-uranyl carbonate mineral
349 kamotoite-(Y). *Mineralogical Magazine*, **81**, 653–660.
350 Pouchou, J.-L. and Pichoir, F. (1991) Quantitative analysis of homogeneous or stratified
351 microvolumes applying the model "PAP." In: Heinrich, K.F.J. and Newbury, D.E. (eds)
352 *Electron Probe Quantitation*. Plenum Press, New York, pp. 3l–75.
353 Saini, R.D., Bhattacharyya, P.K., and Iyer, R.M. (1989) Photoluminescence studies of the
354 uranyl carbonate system. *Journal of Photochemistry and Photobiology, A: Chemistry*, **47**,
355 65–81.
356 Sheldrick, G.M. (2015) Crystal structure refinement with SHELXL. *Acta Crystallographica*,
357 **C71**, 3–8.
358

359 FIGURE CAPTIONS

360 Figure 1. Meyrowitzite on asphaltum. The field of view is 0.5 mm across.

361 Figure 2. Crystal drawing of meyrowitzite, clinographic projection in nonstandard
362 orientation, **b** vertical.

363 Figure 3. Raman spectrum of meyrowitzite recorded using a 785 nm diode laser.

364 Figure 4. Comparison of powder X-ray diffraction patterns for meyrowitzite and zellerite.

365 Figure 5. The uranyl carbonate sheet in the structure of meyrowitzite viewed down [10-1].

366 Figure 6. The structure of meyrowitzite viewed down [010]. The O atoms of isolated H_2O
367 groups are shown as white balls. The unit cell outline is shown by dashed lines.

368 Figure 7. The structure of meyrowitzite viewed down [100]. The O atoms of isolated H_2O
369 groups are shown as white balls. The unit cell outline is shown by dashed lines.

370

371

This is a preprint, the final version is subject to change, of the American Mineralogist (MSA)
Cite as Authors (Year) Title. American Mineralogist, in press.
DOI: https://doi.org/10.2138/am-2019-6814

372 Table 1. Analytical results for meyrowitzite.

Constituent	**Mean**	**Range**	**Stand. Dev.**	**Probe Standard**	**Normalized**
CaO	12.67	12.51–12.93	0.22	diopside	10.18
UO_3	68.77	68.14–69.86	0.95	syn. UO_2	55.23
CO_2*					17.00
H_2O*					17.60
Total					100.01

373 * based on structure.

374

This is a preprint, the final version is subject to change, of the American Mineralogist (MSA)
Cite as Authors (Year) Title. American Mineralogist, in press.
DOI: https://doi.org/10.2138/am-2019-6814

Table 2. Powder X-ray data (d in Å) for meyrowitzite. Only calculated lines with $I \geq 10$ are listed.

I_{obs}	d_{obs}	d_{calc}	I_{calc}	hkl
100	12.11	53	12.3263	0 1 1
		47	11.7651	-1 0 1
48	9.52	24	9.5916	0 0 2
		27	9.4964	-1 1 1
59	8.19	54	8.2383	0 1 2
20	7.74	26	7.7718	-1 1 2
68	5.96	17	6.0527	1 1 2
		51	5.9603	-1 2 2
		26	5.8826	-2 0 2
15	5.54	32	5.5357	2 1 0
		18	5.1643	0 3 1
79	5.04	19	5.0709	1 2 2
		18	5.0604	-1 2 3
30	4.77	52	5.0186	1 0 3
		34	4.7908	1 1 3
		12	4.5898	-1 3 2
45	4.359	46	4.3721	2 2 1
		22	4.3614	-2 2 3
		12	4.2784	-2 1 4
21	4.195	22	4.2491	-1 2 4
		20	4.1448	1 3 2
32	4.057	21	4.1033	-3 0 1
		19	4.0524	-2 3 1
		24	4.0217	0 4 0
31	3.944	17	3.9760	-3 1 1
		20	3.9361	0 4 1
		19	3.9217	-3 0 3
16	3.801	18	3.8101	-3 1 3
		15	3.8055	-1 4 1
27	3.652	16	3.6586	-1 3 4
		20	3.6528	-3 2 2
23	3.368	11	3.3721	-2 4 1
		29	3.3604	1 0 5
19	3.294	17	3.3200	-2 4 2
		10	3.3069	-3 2 4
		16	3.2894	1 1 5
		15	3.2551	-2 0 6
25	3.118	13	3.1383	1 4 3
		11	3.1202	0 3 5
15	2.989	13	3.0047	-3 3 4
		19	2.9711	0 2 6
26	2.852	20	2.8710	-3 4 2
		15	2.8486	1 4 4
		11	2.8452	-1 4 5
		14	2.8242	2 5 0
10	2.763	16	2.7557	-2 4 5
18	2.690	26	2.6821	2 2 5
12	2.636	13	2.6529	-4 3 3
		26	2.6283	-4 2 5
21	2.593	20	2.6044	4 0 2
		24	2.5940	0 2 7
12	2.534	14	2.5328	3 2 4
		15	2.5302	-2 4 6
		10	2.5070	-2 3 7
24	2.476	38	2.4791	-1 6 3
		10	2.4745	4 3 1
9	2.380	23	2.4406	2 6 0
		16	2.3890	3 3 4
13	2.292	23	2.2962	-3 2 8
		10	2.2630	5 2 0
10	2.224	12	2.2439	-5 3 2
		15	2.2187	-1 0 9
13	2.185	12	2.1861	4 4 2
		12	2.1824	3 5 3
6	2.143	15	2.1370	-5 0 7
12	2.0782	14	2.0884	-1 7 4
		12	2.0691	4 4 3
16	2.0482	12	2.0544	0 6 6
		24	2.0500	-6 0 4
22	2.0006	20	2.0176	2 0 8
		10	2.0129	-2 0 10
		29	1.9999	0 8 1
20	1.9662	13	1.9827	-3 7 3
		10	1.9814	-4 6 4
		14	1.9790	1 1 9
		11	1.9587	-1 6 7
15	1.8847	10	1.8988	4 0 6
		14	1.8871	-5 4 7
		15	1.8862	-6 3 5
27	1.8087	17	1.8264	-6 4 4
		20	1.8054	-3 8 2
		10	1.8034	2 4 8
		26	1.8013	-5 6 1
		25	1.7998	1 8 4
26	1.7835	10	1.7901	3 6 5
		11	1.7848	-1 4 10
		12	1.7756	-2 8 5
18	1.7171	12	1.7243	-7 0 1
		19	1.7175	3 8 2
		13	1.7121	-7 2 2
11	1.6771	10	1.6868	-3 6 9
		10	1.6833	-7 2 6
13	1.6282	13	1.6312	4 8 1
		10	1.6276	-4 0 12

This is a preprint, the final version is subject to change, of the American Mineralogist (MSA)
Cite as Authors (Year) Title. American Mineralogist, in press.
DOI: https://doi.org/10.2138/am-2019-6814

Table 3. Data collection and structure refinement details for meyrowitzite.

Diffractometer	Rigaku R-Axis Rapid II
X-ray radiation/power	Mo$K\alpha$ (λ = 0.71075 Å)/50 kV, 40 mA
Temperature	293(2) K
Structural Formula	$Ca(UO_2)(CO_3)_2 \cdot 5H_2O$
Space group	$P2_1/n$
Unit cell dimensions	a = 12.376(3) Å
	b = 16.0867(14) Å
	c = 20.1340(17) Å
	β = 107.679(13)°
V	3819.3(12) Å^3
Z	12
Density (for above formula)	2.714 g cm^{-3}
Absorption coefficient	13.207 mm^{-1}
F(000)	2796
Crystal size	80 × 80 × 30 μm
θ range	3.07 to 22.44°
Index ranges	$-13 \le h \le 13$, $-17 \le k \le 16$, $-21 \le l \le 21$
Frames collected / exposure	36 / 25 min.
Reflections collected / unique	17068 / 4874; R_{int} = 0.085
Reflections with $I > 2\sigma I$	3559
Completeness to θ = 27.48°	98.1%
Refinement method	Full-matrix least-squares on F^2
Parameter / restraints	459/0
GoF	1.052
Final R indices [$I > 2\sigma I$]	R_1 = 0.0553, wR_2 = 0.1296
R indices (all data)	R_1 = 0.0818, wR_2 = 0.1469
Largest diff. peak/hole	+2.05/–1.37 e A^{-3}

$R_{int} = \Sigma|F_o^2 - F_o^2(\text{mean})|/\Sigma[F_o^2]$. GoF = $S = \{\Sigma[w(F_o^2 - F_c^2)^2]/(n-p)\}^{1/2}$. $R_1 = \Sigma||F_o| - |F_c||/\Sigma|F_o|$. $wR_2 = \{\Sigma[w(F_o^2 - F_c^2)^2]/\Sigma[w(F_o^2)^2]\}^{1/2}$; $w = 1/[\sigma^2(F_o^2) + (aP)^2 + bP]$ where a is 0.057, b is 98.855 and P is $[2F_c^2 + \text{Max}(F_o^2, 0)]/3$.

This is a preprint, the final version is subject to change, of the American Mineralogist (MSA)
Cite as Authors (Year) Title. American Mineralogist, in press.
DOI: https://doi.org/10.2138/am-2019-6814

Table 4. Atom coordinates and displacement parameters ($Å^2$) for meyrowitzite.

	x/*a*	*y*/*b*	*z*/*c*	U_{eq}	U^{11}	U^{22}	U^{33}	U^{23}	U^{13}	U^{12}
Ca1	0.7593(4)	0.3457(2)	0.7368(2)	0.0290(10)	0.036(3)	0.019(2)	0.030(2)	0.0017(18)	0.0074(19)	0.0002(18)
Ca2	0.6749(4)	0.5508(2)	0.4255(2)	0.0331(10)	0.046(3)	0.018(2)	0.039(2)	0.0028(19)	0.019(2)	0.0009(19)
Ca3	0.1484(5)	0.1091(3)	0.6308(3)	0.0581(14)	0.075(4)	0.030(3)	0.080(4)	-0.001(3)	0.040(3)	0.005(3)
U1	0.60111(7)	0.34393(4)	0.52659(4)	0.0276(2)	0.0375(5)	0.0153(4)	0.0270(4)	0.0009(3)	0.0054(4)	-0.0003(3)
U2	0.05568(7)	0.33897(5)	0.68741(5)	0.0377(3)	0.0420(6)	0.0198(4)	0.0570(6)	-0.0047(4)	0.0237(4)	-0.0035(4)
U3	0.76212(6)	0.59814(4)	0.74902(4)	0.0262(2)	0.0357(5)	0.0129(4)	0.0273(4)	-0.0021(3)	0.0056(3)	0.0001(3)
C1	0.5974(16)	0.1959(12)	0.6060(10)	0.028(5)	0.031(13)	0.025(12)	0.023(11)	0.015(10)	0.000(9)	-0.018(9)
C2	0.5142(19)	0.6277(15)	0.6177(11)	0.042(6)	0.044(15)	0.049(15)	0.027(13)	-0.015(12)	0.001(11)	-0.002(12)
C3	0.7143(18)	0.4874(12)	0.6019(11)	0.035(5)	0.037(14)	0.020(12)	0.034(13)	-0.008(11)	-0.012(10)	0.006(10)
C4	0.9818(18)	0.4932(12)	0.7280(10)	0.031(5)	0.033(14)	0.028(13)	0.032(12)	0.001(10)	0.008(10)	-0.012(10)
C5	0.253(2)	0.3137(14)	0.6425(13)	0.051(7)	0.058(18)	0.033(14)	0.068(17)	-0.010(12)	0.027(14)	-0.020(13)
C6	0.5804(19)	0.6933(13)	0.8124(12)	0.040(6)	0.033(15)	0.026(13)	0.059(15)	-0.006(11)	0.012(12)	0.006(11)
O1	0.8909(12)	0.6293(7)	0.8609(7)	0.039(4)	0.059(10)	0.008(7)	0.041(8)	-0.013(6)	0.003(7)	0.014(6)
O2	0.5428(13)	0.2016(8)	0.5410(7)	0.042(4)	0.066(11)	0.020(7)	0.035(9)	0.001(7)	0.009(8)	-0.014(7)
O3	0.6485(12)	0.2641(7)	0.6336(6)	0.036(4)	0.058(10)	0.016(7)	0.024(7)	0.016(6)	-0.004(7)	-0.005(7)
O4	0.5196(13)	0.6974(8)	0.5892(7)	0.040(4)	0.060(11)	0.025(8)	0.030(8)	0.003(7)	0.005(7)	-0.012(7)
O5	0.5694(10)	0.6083(8)	0.6814(7)	0.034(3)	0.016(7)	0.030(8)	0.047(9)	0.015(7)	-0.002(7)	-0.008(6)
O6	0.4405(12)	0.5750(8)	0.5799(6)	0.035(3)	0.043(9)	0.029(8)	0.028(8)	0.004(7)	0.003(7)	-0.008(7)
O7	0.7502(12)	0.5550(7)	0.6335(6)	0.034(3)	0.062(10)	0.009(7)	0.029(7)	-0.002(6)	0.013(7)	0.002(6)
O8	0.6969(12)	0.4220(8)	0.6329(6)	0.036(4)	0.068(11)	0.014(7)	0.020(7)	-0.006(6)	0.006(7)	-0.024(7)
O9	0.6874(12)	0.4815(8)	0.5351(6)	0.034(3)	0.054(10)	0.024(7)	0.022(8)	-0.010(6)	0.008(7)	-0.003(7)
O10	0.0716(13)	0.4899(8)	0.7085(8)	0.047(4)	0.051(11)	0.025(8)	0.069(11)	-0.009(7)	0.024(9)	-0.005(7)
O11	0.9489(12)	0.5639(8)	0.7482(8)	0.042(4)	0.044(10)	0.011(7)	0.070(11)	0.003(7)	0.014(8)	0.009(6)
O12	0.9290(12)	0.4250(8)	0.7304(8)	0.044(4)	0.045(10)	0.023(8)	0.071(11)	-0.009(8)	0.029(8)	0.005(7)
O13	1.3390(14)	0.3058(9)	0.6225(8)	0.052(4)	0.056(11)	0.035(9)	0.079(12)	0.018(8)	0.041(10)	0.010(8)
O14	0.1918(13)	0.2544(9)	0.6539(9)	0.052(4)	0.046(10)	0.033(9)	0.095(13)	-0.006(9)	0.048(10)	-0.003(8)
O15	0.2133(13)	0.3884(8)	0.6514(8)	0.045(4)	0.056(10)	0.014(7)	0.077(11)	-0.001(7)	0.039(9)	0.002(7)
O16	0.6442(12)	0.6321(8)	0.8209(7)	0.037(4)	0.039(9)	0.025(8)	0.051(9)	0.006(7)	0.022(7)	0.010(7)
O17	0.9005(12)	0.2643(8)	0.7108(8)	0.045(4)	0.043(10)	0.025(9)	0.074(11)	-0.015(8)	0.031(8)	-0.013(7)
O18	0.0126(13)	0.1893(8)	0.6706(9)	0.050(4)	0.036(10)	0.020(8)	0.104(13)	-0.010(8)	0.036(9)	-0.013(7)
O19	0.7239(12)	0.3057(8)	0.5103(7)	0.038(4)	0.040(9)	0.031(8)	0.041(8)	-0.015(7)	0.007(7)	-0.008(7)

O20	0.4758(12)	0.3843(9)	0.5419(7)	0.041(4)	0.047(10)	0.041(9)	0.034(8)	0.005(7)	0.014(7)	-0.001(7)
O21	0.1367(14)	0.3260(8)	0.7743(8)	0.052(4)	0.068(12)	0.017(8)	0.076(11)	-0.008(8)	0.032(9)	0.001(7)
O22	0.9722(14)	0.3546(9)	0.5997(8)	0.052(4)	0.063(12)	0.036(9)	0.057(10)	-0.007(8)	0.020(9)	-0.016(8)
O23	0.7814(12)	0.7007(7)	0.7220(7)	0.038(4)	0.056(10)	0.009(7)	0.047(9)	0.005(6)	0.011(8)	0.005(6)
O24	0.7443(11)	0.4941(7)	0.7771(6)	0.026(3)	0.039(9)	0.011(6)	0.021(7)	-0.002(5)	0.000(6)	0.001(6)
OW1	0.8697(14)	0.3414(8)	0.8553(7)	0.050(4)	0.077(12)	0.021(8)	0.044(9)	-0.005(7)	0.008(8)	0.014(8)
OW2	0.4310(12)	0.4793(9)	0.6980(7)	0.039(4)	0.034(9)	0.042(9)	0.043(9)	-0.003(7)	0.015(7)	-0.006(7)
OW3	0.5835(14)	0.3514(9)	0.7589(9)	0.060(5)	0.056(11)	0.037(9)	0.097(13)	0.013(9)	0.040(10)	0.004(8)
OW4	0.7873(15)	0.6445(10)	0.5215(9)	0.069(5)	0.065(13)	0.047(10)	0.076(12)	0.014(9)	-0.005(10)	-0.026(9)
OW5	0.2297(14)	0.0784(11)	0.7529(9)	0.071(5)	0.058(12)	0.073(13)	0.091(14)	0.030(11)	0.034(10)	0.017(10)
OW6	0.3441(18)	0.1329(14)	0.6280(13)	0.102(8)	0.089(17)	0.094(16)	0.15(2)	-0.015(15)	0.082(16)	0.000(13)
OW7	0.981(2)	0.0218(13)	0.6179(14)	0.116(9)	0.099(18)	0.075(14)	0.19(3)	-0.056(16)	0.074(17)	-0.031(13)
OW8	0.832(2)	0.4624(15)	0.4427(15)	0.130(9)	0.11(2)	0.100(18)	0.18(3)	-0.006(18)	0.032(18)	0.043(16)
OW9	0.225(3)	-0.0284(16)	0.6251(17)	0.162(12)	0.21(3)	0.082(18)	0.21(3)	-0.031(19)	0.08(3)	0.05(2)
OW10	0.455(3)	0.2152(16)	0.7872(19)	0.166(13)	0.15(3)	0.080(18)	0.29(4)	0.00(2)	0.10(3)	-0.014(18)
OW11	0.241(4)	0.1914(18)	0.8534(16)	0.193(16)	0.31(5)	0.10(2)	0.14(3)	0.027(19)	0.02(3)	0.08(3)
OW12	0.505(3)	0.0168(16)	0.4186(17)	0.199(18)	0.24(4)	0.086(19)	0.18(3)	0.00(2)	-0.07(3)	-0.05(2)
OW13	0.290(3)	0.1861(15)	0.4748(15)	0.141(11)	0.21(3)	0.079(17)	0.16(3)	-0.001(17)	0.10(2)	-0.019(18)
OW14*	0.966(5)	0.325(3)	0.465(3)	0.127(18)						
OW15*	0.011(7)	0.186(5)	0.517(4)	0.21(3)						
OW16*	0.101(5)	0.128(4)	0.514(3)	0.14(2)						
OW17*	0.046(7)	0.160(5)	0.374(4)	0.20(3)						

* 0.5 assigned occupancy.

This is a preprint, the final version is subject to change, of the American Mineralogist (MSA)
Cite as Authors (Year) Title. American Mineralogist, in press.
DOI: https://doi.org/10.2138/am-2019-6814

Table 5. Selected bond distances (Å) for meyrowitzite.

Ca1–O8	2.345(13)	Ca2–OW8	2.35(2)	Ca3–OW16	2.27(5)
Ca1–OW3	2.351(16)	Ca2–O20	2.396(15)	Ca3–OW5	2.409(18)
Ca1–OW1	2.362(15)	Ca2–O9	2.435(13)	Ca3–O14	2.412(15)
Ca1–O17	2.365(15)	Ca2–O6	2.461(14)	Ca3–OW9	2.43(2)
Ca1–O3	2.489(13)	Ca2–OW2	2.482(14)	Ca3–O18	2.439(16)
Ca1–O12	2.494(15)	Ca2–O13	2.487(15)	Ca3–OW7	2.45(2)
Ca1–O24	2.546(12)	Ca2–OW4	2.512(17)	Ca3–OW6	2.47(2)
Ca1–O23	2.575(13)	Ca2–O15	2.565(14)	Ca3–OW15	2.81(8)
<Ca1–O>	2.441	<Ca2–O>	2.461	<Ca3–O>	2.461
U1–O19	1.760(14)	U2–O21	1.745(17)	U3–O23	1.775(12)
U1–O20	1.792(14)	U2–O22	1.773(16)	U3–O24	1.801(11)
U1–O3	2.422(11)	U2–O15	2.412(14)	U3–O5	2.366(12)
U1–O6	2.428(12)	U2–O14	2.415(14)	U3–O11	2.382(14)
U1–O9	2.440(13)	U2–O17	2.430(13)	U3–O1	2.385(13)
U1–O2	2.444(13)	U2–O12	2.438(13)	U3–O7	2.388(12)
U1–O4	2.448(13)	U2–O10	2.463(13)	U3–O16	2.410(13)
U1–O8	2.454(11)	U2–O18	2.467(13)	<U3–O_{Ur}>	1.788
<U1–O_{Ur}>	1.776	<U2–O_{Ur}>	1.759	<U3–O_{eq}>	2.386
<U1–O_{eq}>	2.439	<U2–O_{eq}>	2.438		
C1–O1	1.25(2)	C2–O4	1.27(3)	C3–O7	1.27(2)
C1–O2	1.28(2)	C2–O5	1.29(2)	C3–O8	1.27(2)
C1–O3	1.30(2)	C2–O6	1.31(2)	C3–O9	1.29(2)
<C1–O>	1.28	<C2–O>	1.29	<C3–O>	1.28
C4–O12	1.29(2)	C5–O13	1.25(3)	C6–O16	1.24(2)
C4–O10	1.29(2)	C5–O14	1.28(3)	C6–O17	1.28(2)
C4–O11	1.31(2)	C5–O15	1.33(3)	C6–O18	1.30(3)
<C4–O>	1.30	<C5–O>	1.29	<C6–O>	1.27

This is a preprint, the final version is subject to change, of the American Mineralogist (MSA)
Cite as Authors (Year) Title. American Mineralogist, in press.
DOI: https://doi.org/10.2138/am-2019-6814

Table 6. Bond-valence analysis for meyrowitzite. Values are expressed in valence units.*

	Ca1	Ca2	Ca3	U1	U2	U3	C1	C2	C3	C4	C5	C6	H bonds	Σ
O1						0.53	1.46						0.18	2.17
O2				0.47			1.35						0.13	1.94
O3	0.23			0.49			1.28							1.99
O4				0.47				1.38					0.20	2.05
O5						0.55		1.31					0.19	2.05
O6		0.24		0.48				1.24						1.97
O7						0.52			1.38				0.17	2.08
O8	0.34			0.46					1.38					2.18
O9		0.26		0.47					1.31					2.05
O10					0.45					1.31			0.21	1.97
O11						0.53				1.31			0.16	1.99
O12	0.22				0.47					1.24				1.94
O13		0.23									1.46		0.19	1.88
O14			0.28		0.50						1.35			2.12
O15		0.18			0.50						1.18		0.13	1.99
O16						0.50						1.50		2.00
O17	0.32				0.48							1.35		2.15
O18			0.26		0.45							1.28		1.98
O19				1.75										1.75
O20		0.29		1.65										1.94
O21					1.80								0.20	2.00
O22					1.71								0.11	1.81
O23	0.18					1.70							0.15	2.03
O24	0.19					1.62							0.13	1.94
OW1	0.32													
OW2		0.23												
OW3	0.33													
OW4		0.21												
OW5			0.28											
OW6			0.24											
OW7			0.25											
OW8		0.33												
OW9			0.27											
OW15			0.05											
OW16			0.21											
Σ	2.13	1.98	1.84	6.24	6.36	5.94	4.08	3.93	4.08	3.86	3.98	4.12		

* Cation–O bond valence parameters are from Gagné and Hawthorne (2015). BVS to OW sites are not included, but hydrogen bond contributions to other O sites are included. Hydrogen-bond strengths based on O–O bond lengths from Ferraris and Ivaldi (1988). The isolated OW sites are not included.

This is a preprint, the final version is subject to change, of the American Mineralogist (MSA)
Cite as Authors (Year) Title. American Mineralogist, in press.
DOI: https://doi.org/10.2138/am-2019-6814

Table 7. Comparative data for meyrowitzite and zellerite.

	Meyrowitzite	Zellerite
Ideal formula	$Ca(UO_2)(CO_3)_2 \cdot 5H_2O$	$Ca(UO_2)(CO_3)_2 \cdot 5H_2O$
Space group	$P2_1/n$	$Pmn2_1$ or $Pmnm$ (probable)
a (Å)	12.376(3)	11.220(15)
b (Å)	16.0867(14)	19.252(16)
c (Å)	20.1340(17)	4.933(16)
β (°)	107.679(13)	
V (Å^3)	3819.3(12)	1065(2)
Z	12	4
$Density_{meas.}$ (g·cm^{-3})	2.70(2)	3.25(1)
Optical character	biaxial (+)	biaxial (+)
α	1.520(2)	1.536(5)
β	1.528(2)	1.559(5)
γ	1.561(2)	1.697(5)
$2V$ (°)	53.0(6)	30–40
Reference	This study	Coleman *et al*., 1966

This is a preprint, the final version is subject to change, of the American Mineralogist (MSA)
Cite as Authors (Year) Title. American Mineralogist, in press.
DOI: https://doi.org/10.2138/am-2019-6814

Figure 1

This is a preprint, the final version is subject to change, of the American Mineralogist (MSA)
Cite as Authors (Year) Title. American Mineralogist, in press.
DOI: https://doi.org/10.2138/am-2019-6814

Figure 2

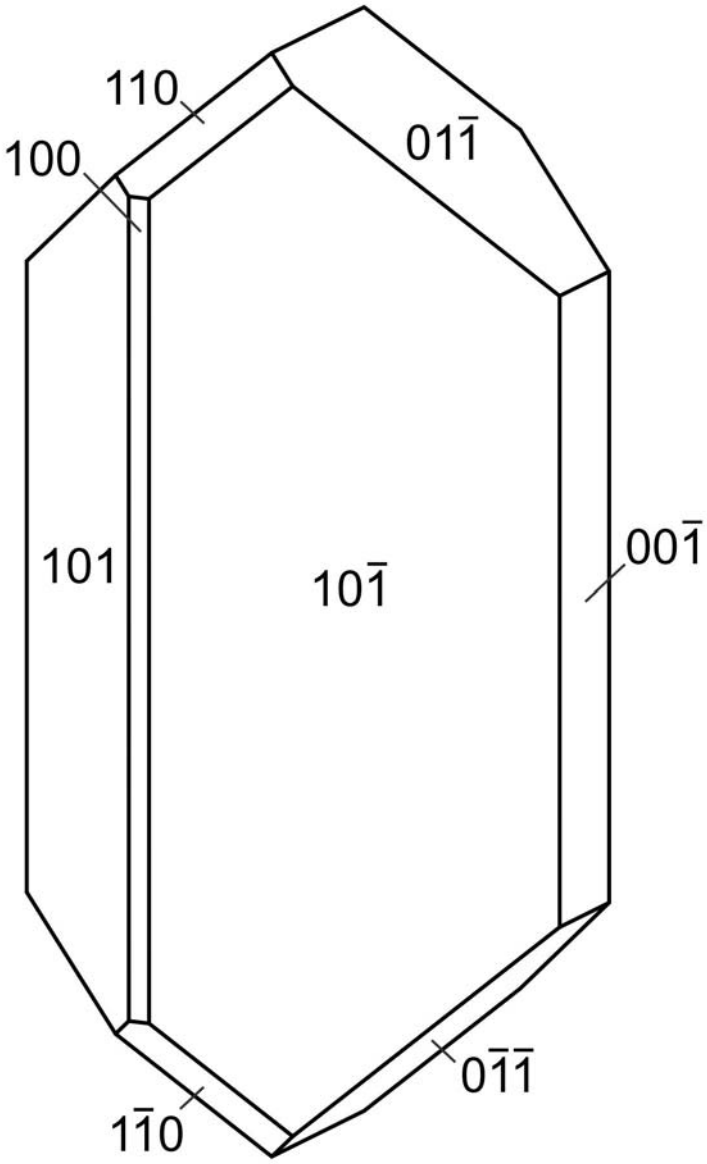

This is a preprint, the final version is subject to change, of the American Mineralogist (MSA)
Cite as Authors (Year) Title. American Mineralogist, in press.
DOI: https://doi.org/10.2138/am-2019-6814

Figure 3

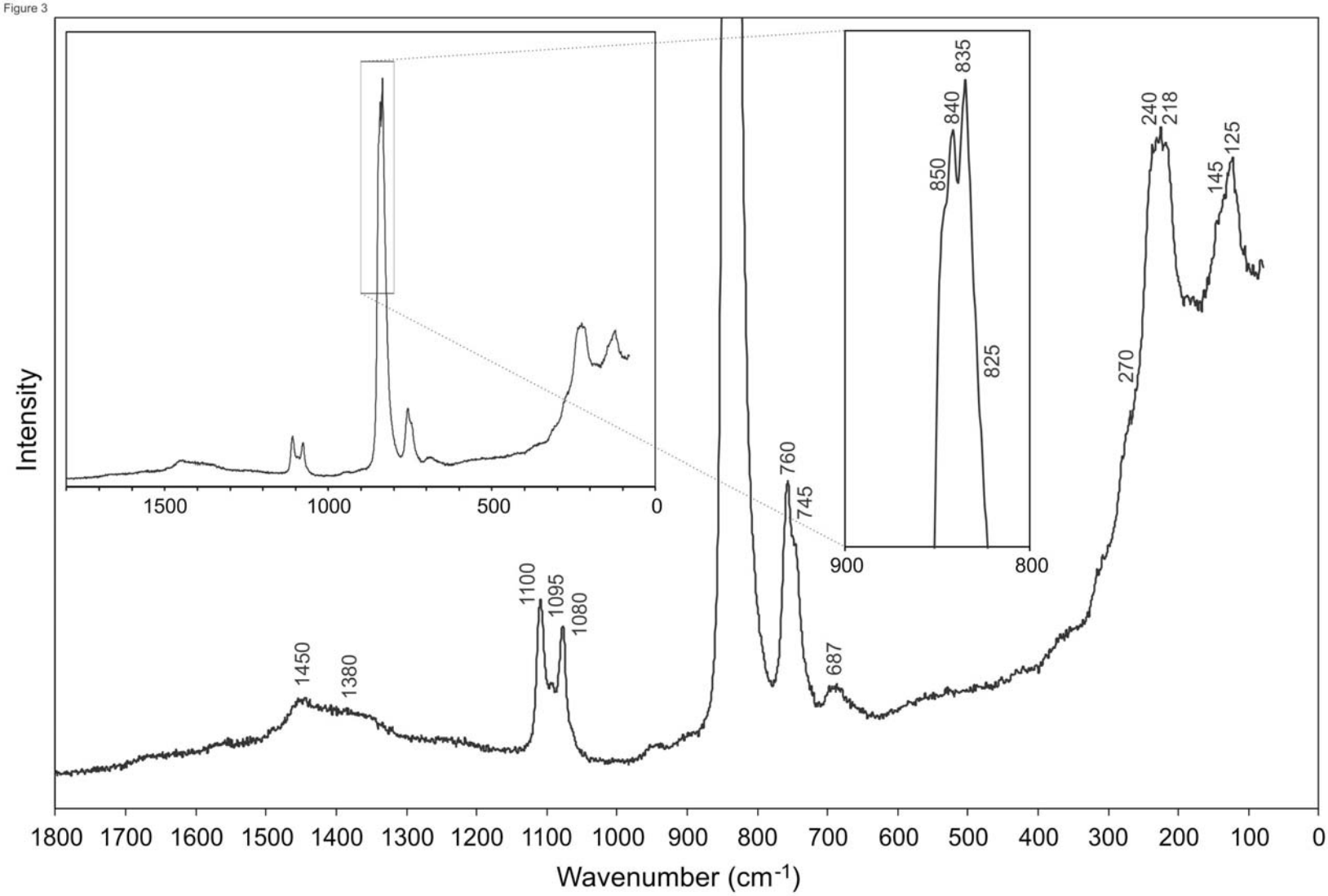

This is a preprint, the final version is subject to change, of the American Mineralogist (MSA)
Cite as Authors (Year) Title. American Mineralogist, in press.
DOI: https://doi.org/10.2138/am-2019-6814

Figure 4

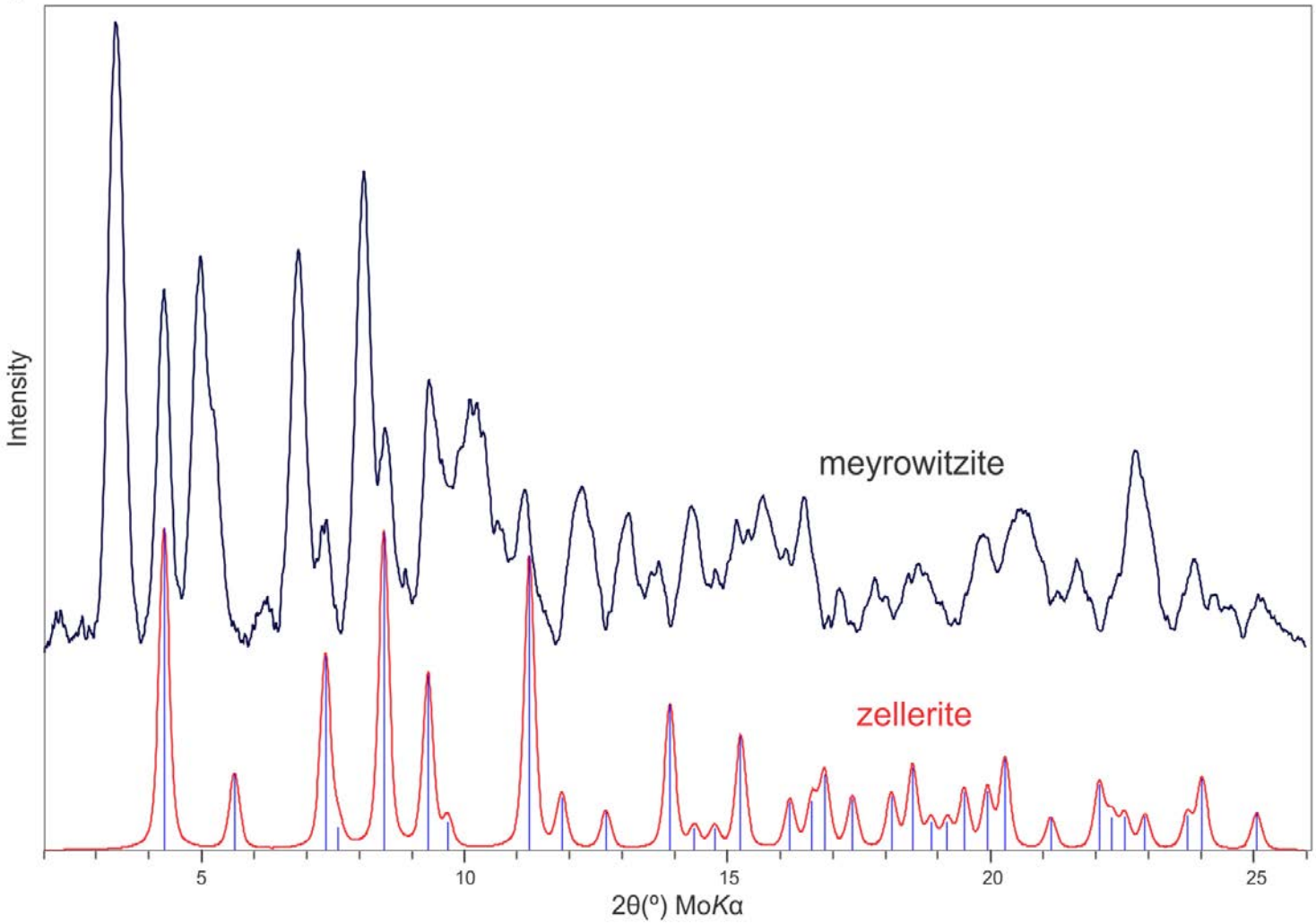

This is a preprint, the final version is subject to change, of the American Mineralogist (MSA)
Cite as Authors (Year) Title. American Mineralogist, in press.
DOI: https://doi.org/10.2138/am-2019-6814

Figure 5

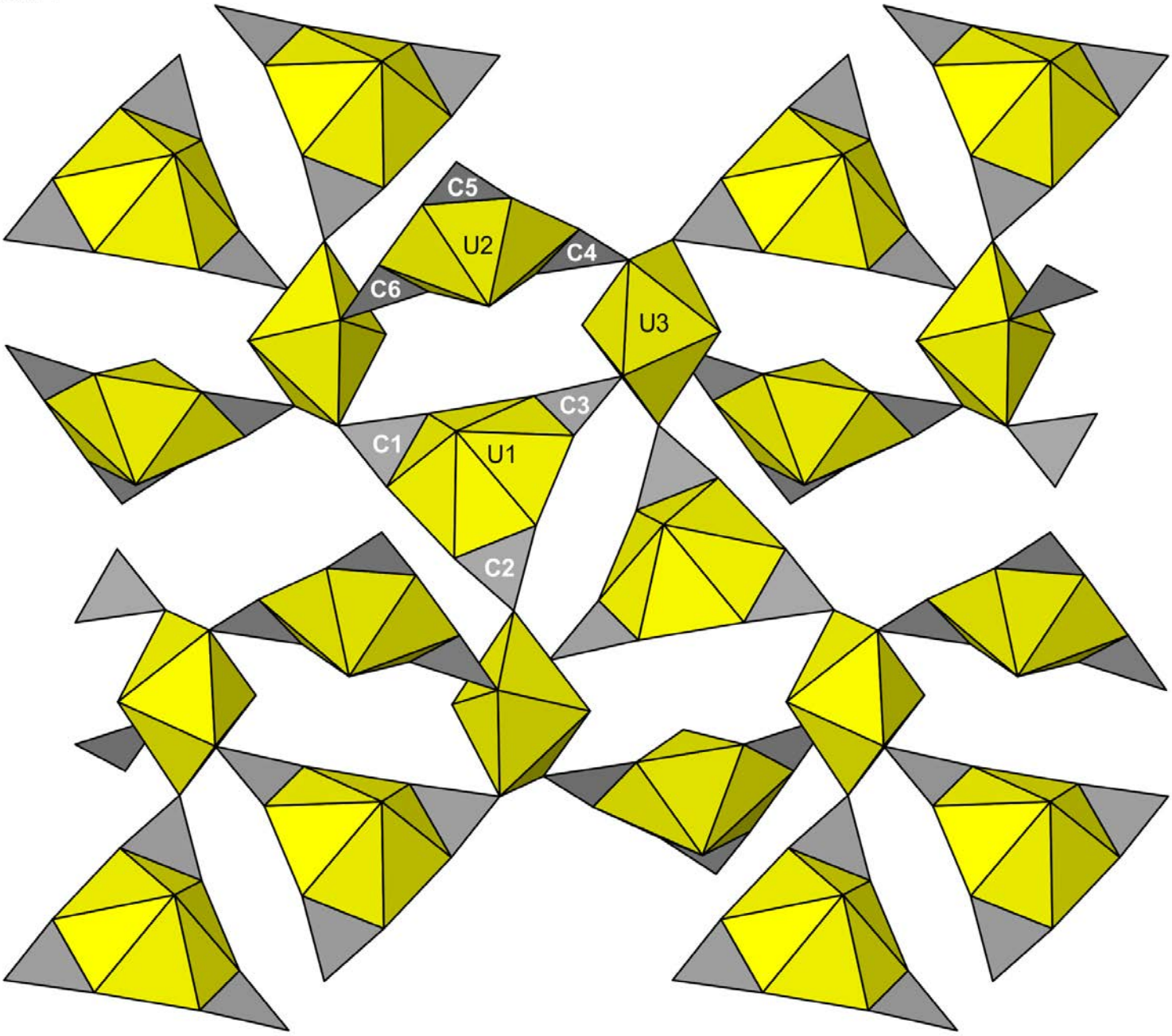

This is a preprint, the final version is subject to change, of the American Mineralogist (MSA)
Cite as Authors (Year) Title. American Mineralogist, in press.
DOI: https://doi.org/10.2138/am-2019-6814

Figure 6

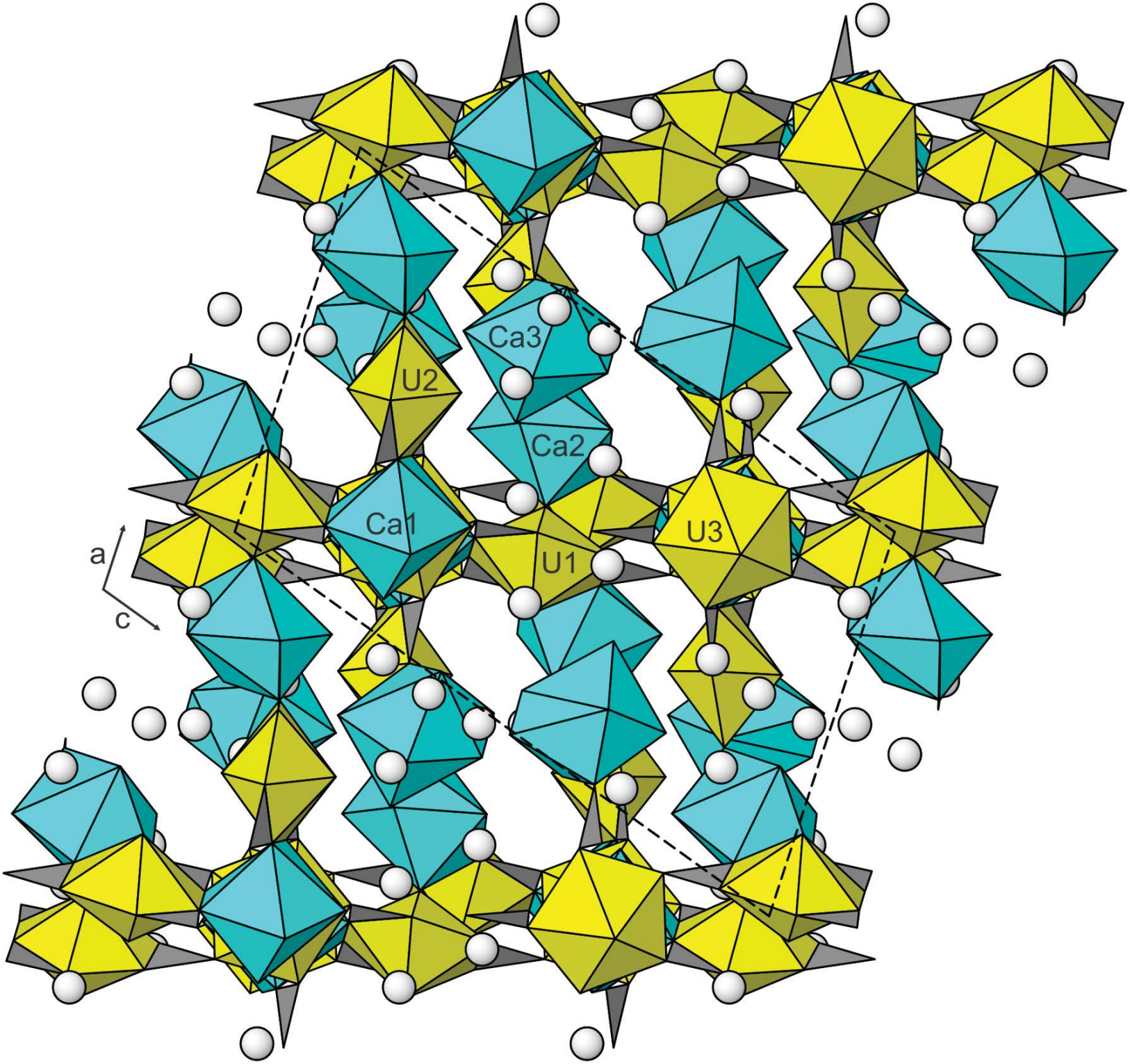

This is a preprint, the final version is subject to change, of the American Mineralogist (MSA)
Cite as Authors (Year) Title. American Mineralogist, in press.
DOI: https://doi.org/10.2138/am-2019-6814

Figure 7